ELSEVIER

Journal of Nuclear Materials 252 (1998) 171–177

journal of nuclear materials

Letter to the Editors

Post-yield strain hardening behavior as a clue to understanding irradiation hardening

R.J. DiMelfi *, D.E. Alexander, L.E. Rehn

Argonne National Laboratory, Argonne, IL 60439, USA

Received 19 May 1997; accepted 29 September 1997

Abstract

We analyze the post-yield true-stress vs. true-strain flow behavior of neutron and electron irradiated reactor pressure vessel steels, A212B and A350, and binary alloys, Fe–0.28 Cu and Fe–0.74 Ni. The flow curves suggest that neutron-irradiation hardening has the same effect as strain hardening for all the materials examined. The post-yield flow curves, obtained after electron-irradiation hardening to yield strength levels similar to those achieved by neutron irradiation, behave differently. © 1998 Elsevier Science B.V.

1. Introduction

Irradiation embrittlement of nuclear reactor pressure vessel steels continues to be of great importance to the energy research community [1]. This is particularly true as life prediction of aging reactors and extension of their licenses become increasingly at issue [2]. Irradiation embrittlement is in fact a reflection of mechanical properties, and, therefore, the mechanical behavior of the material can be used to probe the root causes of embrittlement and serve as a guide as to what to look for and how to model it. One cause of embrittlement is irradiation hardening. In this note, we use the post-yield deformation behavior of irradiated materials to probe the phenomenon of irradiation hardening.

A manifestation of irradiation embrittlement in pressure vessel steels is a shift in the ductile-to-brittle-transition-temperature (DBTT) to higher values, sometimes by as much as 200°C [3], after exposure to displacement-producing radiation. This can bring the brittle fracture regime dangerously close to the reactor operating temperature range. It is widely accepted that the shift to higher transition temperature after irradiation is the result of an overall increase in the yield stress, caused by the interaction between glide dislocations and irradiation-produced point defect clusters. Two of the present authors and their co-workers [4,5] used electron irradiation experiments to study the hardening effects of gamma-ray exposure of reactor pressure vessel steels and binary iron-based alloys (see Table 1). One of their findings was a notable similarity in the yield strength increases produced by electrons and neutrons when compared on a displacements per atom (dpa) basis after irradiations at low temperatures ($T \leq$ 60°C). This observation is consistent with the apparent additivity of the effects of gamma and neutron irradiation, resulting in the 'accelerated' embrittlement of the high flux isotope reactor (HFIR) at Oak Ridge National Laboratory [6,7].

Though explainable in terms of a reaction-rate theory model of defect production and clustering [5,8,9], it is nonetheless surprising and provocative to find that electrons and neutrons affect the yield strength in very much the same way. Because of the likely difference in damage produced by these different kinds of irradiation, mechanical properties other than yield strength may be affected differently. In this note, we study the post-yield flow behavior as it reflects this difference and provides insight into the nature of irradiation-produced defects and their interaction with glide dislocations. From a practical standpoint, different post-yield flow behaviors can have important consequences with regard to pressure vessel life pre-

* Corresponding author. Tel.: + 1-630 252 3736; fax: + 1-630 252 3075; e-mail: dimelfi@anl.gov.

PII S0022-3115(97)00316-4

Table 1
Elemental compositions of alloys in weight percent

Element	A212B	A350	Fe–0.28Cu	Fe–0.74Ni
C	0.26	0.18	0.013	0.01
Al	0.07	0.08	0.007	< 0.005
Co	0.015	0.03		
Cr	0.075	0.090		
Cu	0.15	0.11	0.28	< 0.005
Mn	0.85	0.55	0.013	0.017
Mo	0.02	0.03		
Nb	< 0.001	< 0.001		
Ni	0.20[a]	3.3	0.012	0.74
Si	0.29	0.29		
Sn	0.02	0.02		
Ti	0.01	< 0.001		
V	0.0005	0.001		
W	< 0.005	< 0.005		
Zr	< 0.001	< 0.001		
P	0.006	0.01	0.004	0.003
S	0.04	0.02		
As	0.007	0.01		
B	< 0.0005	< 0.0005		
N	0.0060	0.0090		
O	0.0024	0.0027		

[a] Believed to be high; independent analysis at another laboratory showed 0.09 wt%.

diction. For example, while the true stress at engineering ultimate, which we will show is different in the steels we examine for different irradiating particles, is unrelated to the DBTT, it is intimately related to fatigue life [10]. Also, our examination of the post-yield flow behavior of different alloys, irradiated with neutrons and electrons, will provide clues about the way different alloy constituents interact with the different kinds of irradiation damage to strengthen the material differently. We discuss below the characteristics of two general strengthening effects that we believe are relevant to the differing defect cluster characters produced by neutrons and electrons in four different alloys: two pressure vessel steels, A212B and A350; and two binary alloys, Fe–0.28 wt% Cu and Fe–0.74 wt% Ni.

2. Analysis

Raw tensile data on the irradiated alloys studied in this paper were provided by Farrell [11]. Refs. [5,6] should be sought for details of the electron and neutron irradiation conditions, respectively. Testing was performed at room temperature at a nominal strain rate of 1.1×10^{-3} s^{-1} [5,6]. Data were obtained from miniature (ASTM SS-3) tensile specimens, and sample extension was extracted from the machine cross head displacement. In the present analysis, we assumed that this reported extension occurred only in the gauge section of the sample. In the case of electron irradiation, this assumption might appear problem-

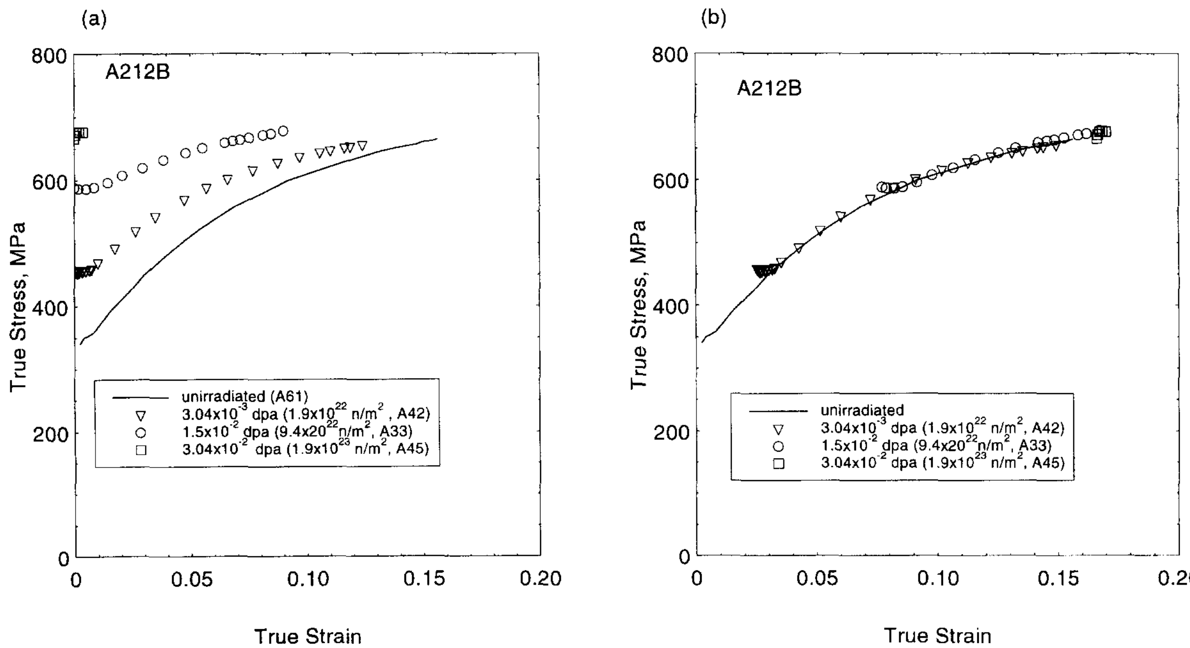

Fig. 1. The true-stress flow curves for neutron irradiated ($T \leq 60$°C) pressure vessel steel A212B to the indicated fluence and corresponding damage levels is shown. In (a) the flow curves are left unshifted and referenced to zero plastic strain in each case. In (b) the curves are shifted along the strain axis so that their yield stress falls on the flow curve for unirradiated material.

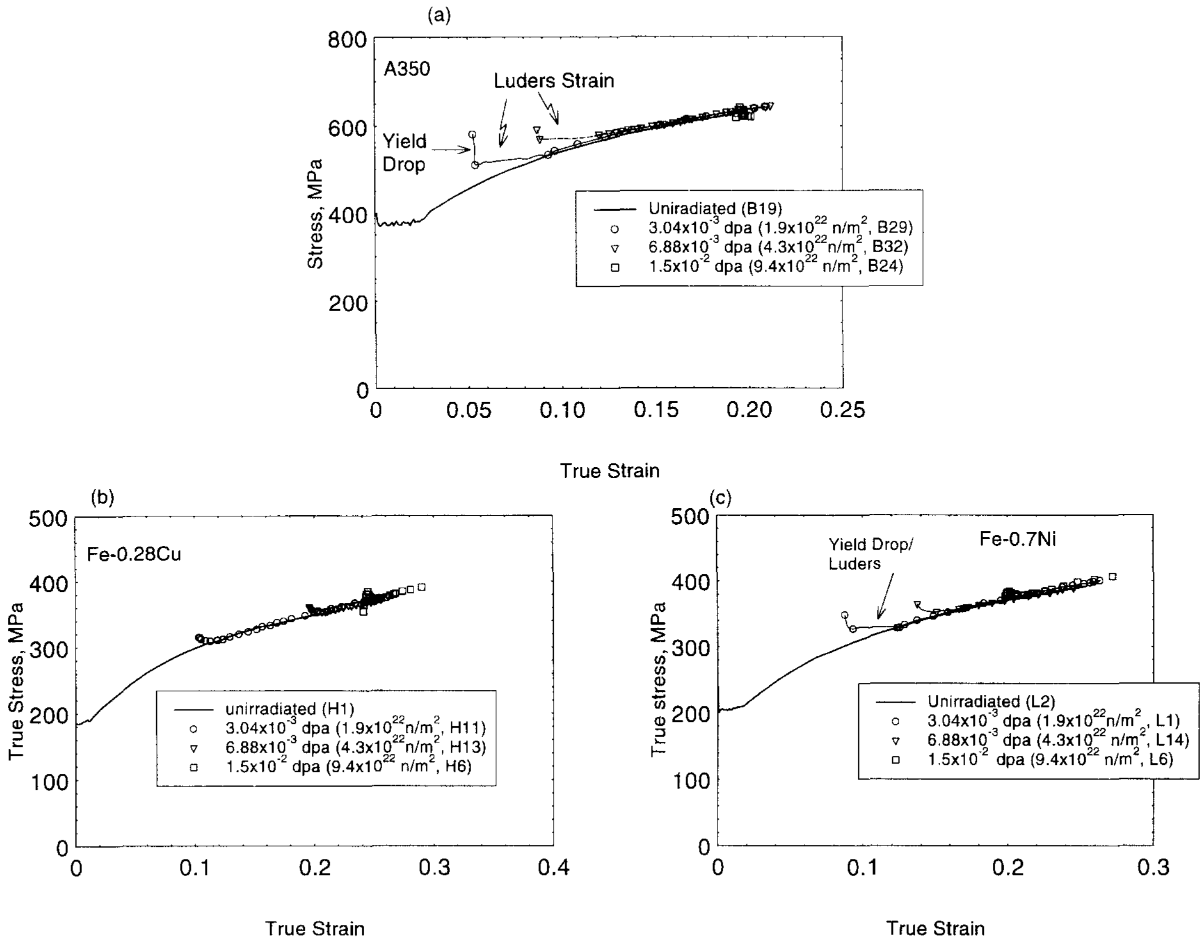

Fig. 2. The true-stress flow curves for neutron irradiated ($T \leq 60°C$) pressure vessel steel A350 (a), Fe–0.28 Cu (b), and Fe–0.74 Ni (c) to the indicated fluence and corresponding damage levels is shown. The flow curves are shifted along the strain axis so that the point where uniform flow begins in each case (after Lüders strain is complete) coincides with the flow curve for unirradiated material.

atic for such small samples because they were irradiated, and, therefore, irradiation-hardened, chiefly in the gauge section. However, post-failure measurements of the very limited plastic flow that occurred outside of the specimen gauge section, and calculations based on these measurements, strongly support this assumption for these samples. Space limitations prevent us from presenting the details here. Throughout this analysis, the true stress is determined from the reported uniform elongation and the assumption of constant volume during plastic flow, and the true strain is determined only to the point of maximum load.

Fig. 1 shows the true-stress vs. true-plastic-strain flow curves extracted from the raw data for A212B, *neutron* irradiated [5] to a range of damage levels expressed in displacements per atom (dpa). Fig. 1a shows the flow behavior for this material for the range of irradiation conditions with each curve referenced to zero plastic strain in each case. Fig. 1b shows the same curves for irradiated material shifted horizontally along the strain axis so that their yield stress lies on the unirradiated curve. When this is done, the flow curves for irradiated material superimpose on the curve for unirradiated material. In this case, the *true* stress at ultimate is essentially the same for both unirradiated samples and samples irradiated over the range of doses indicated. This behavior is consistent with that displayed by true-stress flow curves of neutron irradiated type 316 stainless steel [12], several advanced ferritic and austenitic stainless steels [13] and early data on A212B, similarly exposed [14]. Fig. 2 shows similar behavior for A350 and the Fe–Cu and Fe–Ni binary alloys after the curves for irradiated material have been shifted appropriately along the strain axis.

The true-stress flow curves for the *electron* irradiated A212B samples [5] are shown Fig. 3. In Fig. 3a, the flow curves are shown not shifted, i.e., referenced to zero plastic strain in each case. In Fig. 3b, these curves are shifted horizontally to the right along the strain axis to

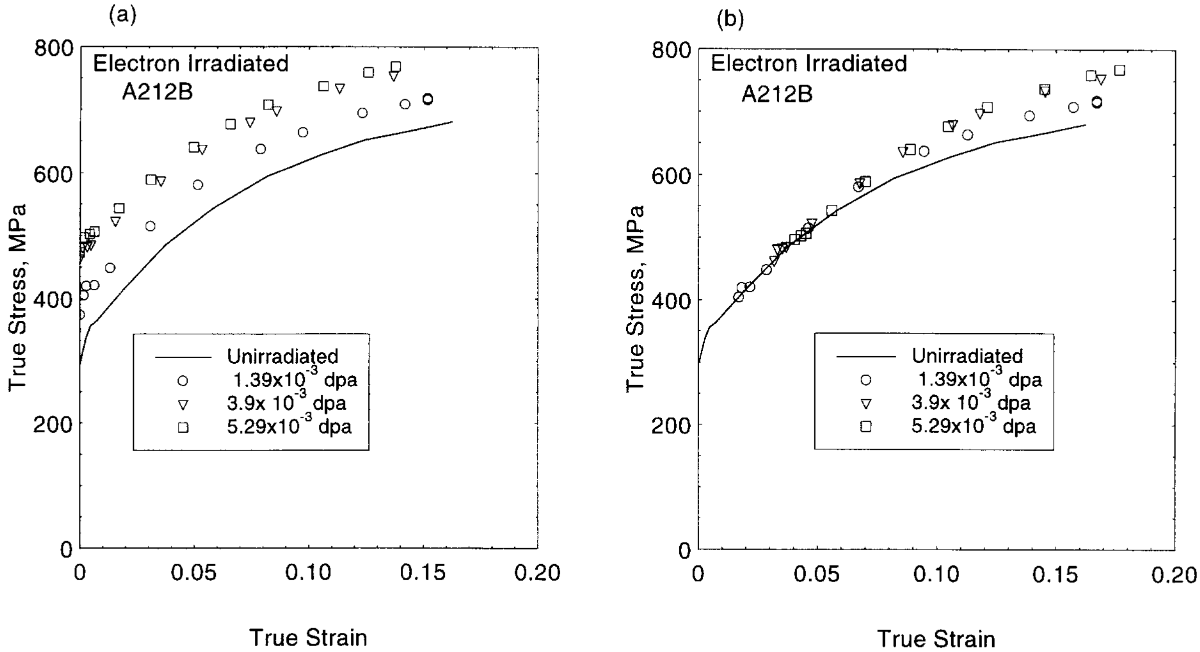

Fig. 3. The true-stress flow curves for electron irradiated (35°C ≤ T ≤ 60°C) pressure vessel steel A212B to the indicated damage levels is shown. In (a) the flow curves are left unshifted and referenced to zero plastic strain in each case. In (b) the curves are shifted along the strain axis so that their yield stress falls on the flow curve for unirradiated material.

points where their yield stress values intersect the same stress level on the unirradiated-sample flow curve. Unlike in the case of neutron exposure, after yielding, the flow curves for electron irradiated A212B continue at higher hardening rates than that of the unirradiated material. For electron irradiation, the true stress at the engineering ultimate strength is greater than that for unirradiated material. This is so, even though, as indicated previously, the yield stress changes after irradiation are quite similar at the same damage level for both neutron and electron irradiation (for irradiations at $T \leq 60°C$). As with the increases in yield strength, the increases in hardening rate at a given stress are systematic with increasing dose. A similar effect is shown in Fig. 4 for A350, where the curves for irradiated material are shifted along the strain axis as described above. The true-stress flow curves for electron irradiated samples of Fe–0.28Cu and Fe–0.74Ni are shown in Fig. 5 after shifting along the strain axis. It is seen in this figure that, for these alloys, the post-yield hardening rate of the electron-irradiated materials is not as clearly different from that of unirradiated materials as it is in the case of the steels. Therefore, for the binary alloys, the post-yield strain-hardening behavior is not very different after irradiation hardening to the same yield strength levels by either electrons or neutrons. These results imply that the putative difference in mechanism that causes the distinct difference between electron and neutron irradiation-strengthening in pressure vessel steels (cf. Section 3) is less prominent in these model alloys.

3. Discussion

The collection of results for both steels and model alloys displayed above indicates that irradiating particle and alloy chemistry are both important to producing a particular kind of strengthening phenomenon. One might expect that the cascade damage caused by neutron irradiation would produce defect clusters that are different in nature from those produced by the more uniformly distributed electron damage, and that this would result in different strengthening effects. It is our contention that the two differing mechanical responses are, in essence, fingerprints of differing defect characteristics.

One way to understand this behavior is to imagine that increases in yield strength are determined by the stress required for glide dislocations to pass the irradiation-produced defect clusters, whatever their nature. This approach and variations on it are what is usually done in analyses of this phenomenon (e.g., [15]). It is difficult to imagine these defect clusters having very different number densities for the two kinds of irradiation in order for them to have the same effect on the yield strength. However, the difference in post-yield flow behavior observed in the irradiated

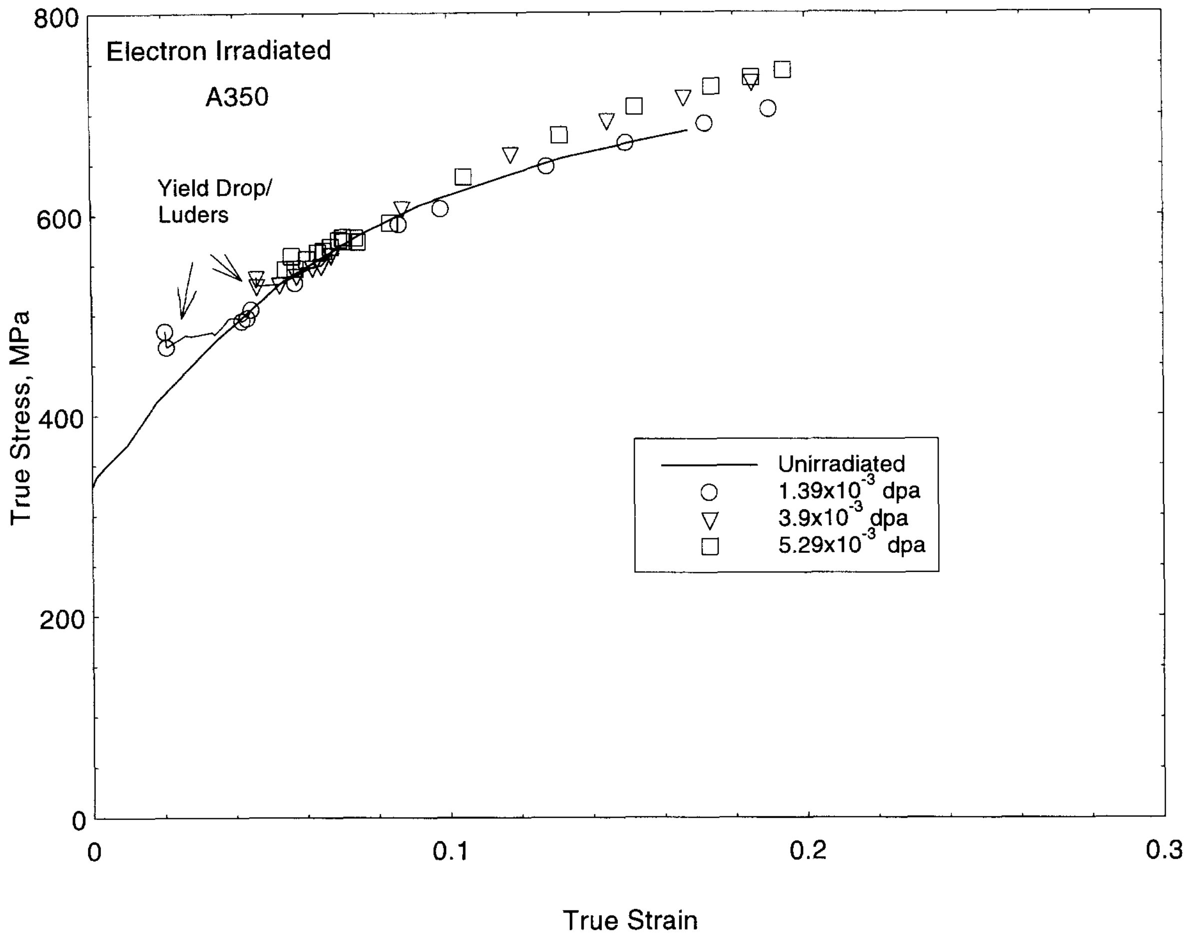

Fig. 4. The true-stress flow curves for electron irradiated (35°C ≤ T ≤ 60°C) pressure vessel steel A350 to the indicated damage levels is shown. The curves are shifted along the strain axis so that their yield stress (after yield drop and/or Lüders strain is complete) falls on the flow curve for unirradiated material.

steels suggests inherent differences in character between those clusters produced by electrons versus those produced by neutrons. The fact that flow behavior differences are not very pronounced in the two model alloys suggests that alloy chemistry is also involved in producing microstructural and mechanical behavior differences in the irradiated steels. This does not mean that we rule out the possible influence of the pressure vessel steel microstructure itself, which, of course, is considerably more complex than that of the binary alloys. However, the low irradiation dose and low irradiation temperatures (< 60°C) discussed here produce a fine-scale distribution of very small defect clusters, which, nonetheless, results in substantial increases in strength over and above the inherent strength of the steels or model alloys, respectively. It is unlikely that, at these low irradiation temperatures, the phases and precipitates in the steel microstructures are altered substantially by the low-dose irradiations [16], so one might be inclined to attribute differing strengthening effects to different solute species. A limited amount of information is available in Ref. [17] on the heat-treat history of these pressure vessel steels for the interested reader.

The exact nature of the defect clusters comprising the irradiated steel microstructure cannot be definitively determined by the current analysis, and, without more direct microstructural evidence, it is inappropriate to speculate about it. However, important clues are present. First, the observation that the flow curves of neutron irradiated steels exhibit, after shifting along the strain axis, a flow behavior similar to unirradiated steels suggests that the defect clusters produced in this case cause a hardening behavior similar to strain hardening. Second, the increased post-yield hardening rate observed for electron irradiated steels indicates that the resulting defect clusters are such that they alter the dislocation multiplication rate after yielding beyond that which can be attributed to normal strain hardening in unirradiated material. Third, the fact that the defect clusters, which produce an increased strain hardening rate, form during electron irradiation and not during neutron irradiation of the steels indicates that both

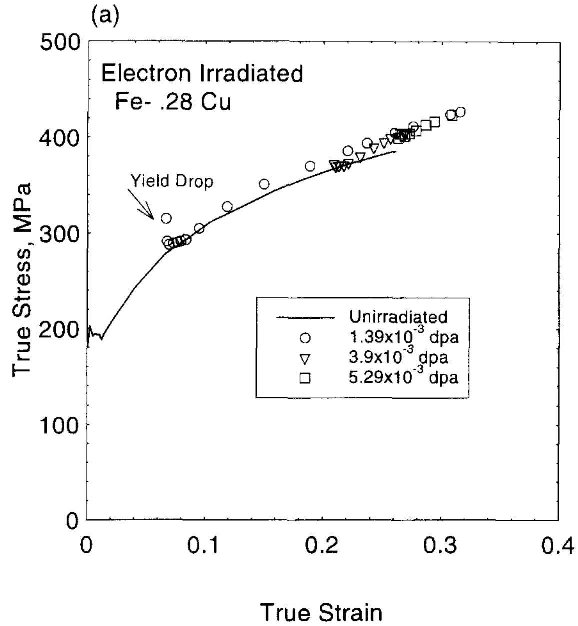

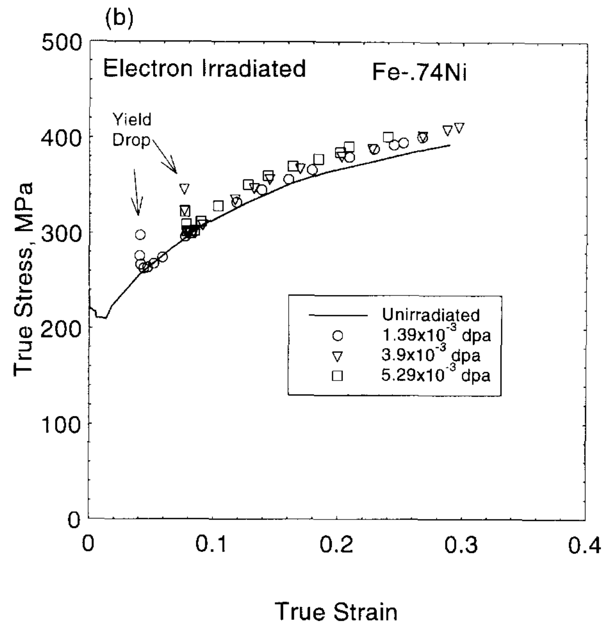

Fig. 5. The true-stress flow curves for electron irradiated (35°C $\leq T \leq$ 60°C) Fe–0.28 Cu (a), and Fe–0.74 Ni (b) to the indicated damage levels is shown. The curves are shifted along the strain axis so that their yield stress (after yield drop and/or Lüders strain is complete) falls on the flow curve for unirradiated material.

the primary damage state and the subsequent interaction of defects with key alloy element(s) in the steels figure importantly in the formation of these defect clusters. Fourth, the more pronounced increase in post-yield hardening rate observed in the electron irradiated steels than in electron-irradiated model alloys implies that alloying element(s), other than or in addition to Cu or Ni, present in the steels, e.g., Mn or C, influence the formation of such defect clusters.

4. Summary and conclusions

In this letter, we have shown that there are differences in the post-irradiation mechanical behavior for the two kinds of irradiation and that the differences are related both to differences in damage produced and alloy chemistry. We have found that, while electron and neutron irradiations (at $T \leq$ 60°C) of pressure vessel steels and binary iron-based model alloys produce similar increases in yield strength for the same dose level, they do not result in the same post-yield hardening behavior. For neutron irradiation, the true-stress flow curves of the irradiated material superimpose on that of the unirradiated material, when the former are shifted appropriately along the strain axis. This behavior suggests that neutron irradiation hardening has the same effect as strain hardening for all of the materials analyzed. For electron irradiated steels, the post-yield hardening rate is clearly greater than that of the unirradiated material, and the flow curves cannot be made to superimpose. The binary iron-base model alloys studied here show a less pronounced difference in flow behavior for neutrons and electrons than exhibited by the steels. A better understanding of these phenomena will come from experiments involving the direct and indirect observation of defects produced by neutrons and electrons in different alloys, and from the mechanistic models engendered by these experiments.

Acknowledgements

The authors gratefully acknowledge Dr Ken Farrell for apprising us of important issues regarding the tensile testing of irradiated small specimens and for providing us with the raw tensile data he obtained, which was used in our analysis. This work was performed under the auspices of the United States Department of Energy and was supported by the US Department of Energy Technology Support Programs and BES-Materials Sciences under Contract No. W-31-109-ENG-38.

References

[1] See, for example, R.E. Gold, A.R. McIlree, S.M. Breuemmer (Eds.), Proc. 7th Int. Symposium on Environmental Degradation of Materials in Nuclear Power Systems — Water Reactors, NACE International, Houston TX, 1995; or G. Tsotridis, R. Dierckx, P. D'Hondt (Eds.), Proc. 7th ASTM-Euratom Symposium on Reactor Dosimetry, Kluwer Academic, Dordrecht, 1992.

[2] Code of Federal Regulations, Requirements for Renewal of Operating Licenses for Nuclear Power Plants, Title 10, Part 54, Sections 1–43, revised Jan. 1, 1996.

[3] D. Pachur, in: D. Kramer, H.R. Brager, J.S. Perrin (Eds.), Proc. 10th Int. Symp. on Effects of Radiation on Materials, ASTM STP 725, Philadelphia, American Society for Testing and Materials, PA, 1981, p. 5.
[4] D.E. Alexander, L.E. Rehn, J. Nucl. Mater. 217 (1994) 213.
[5] D.E. Alexander, L.E. Rehn, K. Farrell, R.E. Stoller, J. Nucl. Mater. 228 (1996) 68.
[6] K. Farrell, S.T. Mahmood, R.E. Stoller, L.K. Mansur, J. Nucl. Mater. 210 (1994) 268.
[7] I. Remec, J.A. Wang, F.R. Kam, K. Farrell, J. Nucl. Mater. 217 (1994) 258.
[8] R.E. Stoller, in: A.S. Kumar, D.S. Gelles, R.K. Nanstad, E.A. Little (Eds.), Effects of Radiation on Materials, ASTM STP 1175, American Society for Testing and Materials, Philadelphia, PA, 1993, p. 394.
[9] R.E. Stoller, in: R.E. Gold, E. Simonen (Eds.), Proc. 6th Int. Symp. on Environmental Degradation of Materials in Nuclear Power Systems — Water Reactors, TMS, Warrendale, PA, 1993, p. 747.
[10] J. Weertman, Int. J. Fracture 2 (1966) 460.
[11] K. Farrell, private communication, 1997.
[12] R.J. DiMelfi, J.M. Kramer, J. Nucl. Mater. 89 (1980) 338.
[13] B. Goshchitskii, V. Sagaradze, private communication under US Russian Agreement #942492402, Report on the Development of Radiation Resistant Alloys, Dec. 1995, Yekaterindurg, Russia.
[14] J.C. Wilson, in: 2nd United Nations Conf. on the Peaceful Uses of Atomic Energy, Geneva, Switzerland, vol. 5, 1958, p. 432; and reported in Radiation Effects on Toughness of Ferritic Steels for Reactor Vessels, An AEC Monograph, L.P. Trudeau, Rowman Littlefield New York, 1964, p. 53.
[15] G.R. Odette, in: M. Davies (Ed.), Neutron Irradiation Effects in Reactor Pressure Vessel Steels and Weldments, IAEA Technical Report Series, Vienna (in press).
[16] Oak Ridge National Laboratory Technical Report ORNL/TM-10444 (DE88 008959), in: R.D. Cheverton, J.G. Merkle, R.K. Nanstad (Eds.), Evaluation of HFIR Pressure-Vessel Integrity Considering Radiation Embrittlement, Apr. 1988 p. 155.
[17] Oak Ridge National Laboratory Technical Report ORNL/TM-10444 (DE88 008959), in: R.D. Cheverton, J.G. Merkle, R.K. Nanstad (Eds.), Evaluation of HFIR Pressure-Vessel Integrity Considering Radiation Embrittlement, Apr. 1988, p. 118.